Biol. Cybern. 90, 318–326 (2004)
DOI 10.1007/s00422-004-0475-5

Biological Cybernetics

Letter to the Editors

Is partial coherence a viable technique for identifying generators of neural oscillations?

Zimbul Albo[⋆], Gonzalo Viana Di Prisco, Yonghong Chen[⋆⋆], Govindan Rangarajan[⋆⋆⋆], Wilson Truccolo[†], Jianfeng Feng[‡], Robert P. Vertes, Mingzhou Ding

Center for Complex Systems and Brain Sciences, Florida Atlantic University, 777 Glades Road, Boca Raton, FL 33431–0991, USA

Received: 26 September 2003 / Accepted: 3 March 2004 / Published online: 16 June 2004

Abstract. Partial coherence measures the linear relationship between two signals after the influence of a third signal has been removed. Gersch proposed in 1970 that partial coherence could be used to identify sources of driving for multivariate time series. This idea, referred to in this paper as Gersch Causality, has received wide acceptance and has been applied extensively to a variety of fields in the signal processing community. Neurobiological data from a given sensor include both the signals of interest and other unrelated processes collectively referred to as measurement noise. We show that partial-coherence-based Gersch Causality is extremely sensitive to signal-to-noise ratio; that is, for a group of three or more simultaneously recorded time series, the time series with the highest signal-to-noise ratio (i.e., relatively noise free) is often identified as the "driver" of the group, irrespective of the true underlying patterns of connectivity. This hypothesis is tested both theoretically and on experimental time series acquired from limbic brain structures during the theta rhythm.

1 Introduction

A single random variable is characterized by its mean and variance. The degree of linear relationship between a pair of random variables is assessed by the correlation coefficient. For three random variables, an additional quantity called partial correlation can be computed that measures the linear relation between a pair of variables after the influence of the third variable has been removed or "partialled out". This assesses whether the correlation between a pair of variables can be fully accounted for by the presence of the third one. Specifically, if the partial correlation between two previously correlated variables is zero, we say that the original correlation is spurious. Similar techniques exist for situations with more than three variables (Bendat and Piersol 1986).

Neurobiological signals are often collected in the form of time series. For multiple time series in the spectral domain, quantities analogous to variance, correlation coefficient, and partial correlation coefficient are spectral power, ordinary coherence, and partial coherence, computed as functions of frequency. It is often the case that symmetric interdependence measures like ordinary coherence are not completely satisfactory, and further partitioning of relationships among a set of simultaneously recorded neural signals is required to parcel out functional connectivity of complex neural networks. Recognizing the potential of partial coherence in achieving this goal, Gersch, in an investigation of identifying epileptic foci using three electrodes, proposed that *"one channel is said to drive the other channels if the first channel explains or accounts for the linear relation between the other two"* (Gersch and Goddard 1970). Here the quantity computed is partial coherence, and we henceforth refer to this partial-coherence-based driver identification approach as Gersch Causality.

Over the years Gersch Causality has been explicitly (or implicitly) employed by many researchers as a way of identifying connectivity, sources of driving, or causal influence. A variety of neurobiological data including EEG signals, multiple spike trains, and unit-EEG mixed recordings have been analyzed using partial coherence (Cohen et al. 1995; Rosenberg et al. 1998; Larsen et al. 2000). Currently, partial coherence analysis and the associated Gersch Causality interpretation is generally perceived as a robust and powerful method for the identification of plausible patterns of neural circuits (Lopes da Silva et al. 1980; Turbes et al. 1983; Turbes and Schneider 1989; Kocsis and Vertes 1994; Halliday et al. 1995; Sherman et al. 1997; Kocsis et al. 1999; Mima et al. 2000; Timmermann et al. 2003; Kubota et al. 2003). For neurobiological data, a complicating factor is that a time

Correspondence to: Mingzhou Ding (e-mail: ding@fau.edu)
⋆ Present address: Department of Neurology, University of Miami School of Medicine, Miami, FL 33101, USA
⋆⋆ On leave from Xi'an Jiaotong University, Xi'an 710049, P.R. China
⋆⋆⋆ Present address: Department of Mathematics and Centre for Theoretical Studies, Indian Institute of Science, Bangalore 560 012, India
† Present address: Department of Neuroscience, Brown University, Providence, RI 02912, USA
‡ Present address: COGS, University of Sussex, Brighton BN1 9QH, UK

series recorded by a sensor inevitably involves a mixture of the signal of interest (e.g., theta oscillations in the hippocampus) and other unrelated processes collectively referred to as measurement noise (Fuller 1987). The effectiveness of partial coherence and Gersch Causality in situations in which biological data consists of signal plus noise is the fundamental question addressed in this paper.

The experimental preparation considered here is the limbic system of the rat during the theta rhythm. Recent evidence suggests that in addition to the hippocampus (Hipp), the anterior thalamus (ATh) and the retrosplenial cortex (RCx) are elements of this system. For instance, we have recently shown that single cells of ATh fire rhythmically, synchronous with the theta rhythm (Vertes et al. 2001; Albo 2003). We have further identified slow rhythmical activity (EEG) at theta frequencies in the RCx and sought to determine the source for the generation of theta in the three structures. In an examination of simultaneous recordings of unit activity from ATh, and EEG signals from the Hipp and RCx of the rat (Albo et al. 2001), we found that the application of partial coherence and Gersch Causality led to contradictory conclusions. We hypothesize that the root of the conflict lies in the degree of noise embedded in each recorded signal; that is, signals with higher signal-to-noise ratios will have disproportionately stronger influence on an interrelated set of signals than those with lower signal-to-noise ratios. We develop this hypothesis by heuristic argument, confirm it using a simulation involving multiple time series configured in a known connectivity pattern, and obtain supporting evidence from the acquired biological data.

2 Methods

2.1 Data acquisition

Experiments were performed on nine male Sprague–Dawley rats (Charles River, Wilmington, MA, USA) weighing 325–450 g in accordance with all federal regulations and National Institutes of Health guidelines for the care and use of laboratory animals and approved by the Florida Atlantic University Institutional Animal Care and Use Committee.

A polyethylene catheter was inserted in the left femoral vein under methoxyflurane anesthesia. The IV administration of urethane (80%) maintained proper levels of anesthesia throughout the duration of the experiment. The level of anesthesia was kept in such a way that the withdrawal reflex was abolished but a gentle tail pinch would elicit the appearance of the hippocampal theta rhythm.

For hippocampal and cortical EEG recordings, two Teflon-coated stainless steel twisted wires (125 μm) separated by 1 mm at the tip were stereotaxically implanted in the left dorsal hippocampus (coordinates: rostrocaudal −7.5, mediolateral 1.5, dorsoventral −3.0) and on the left retrosplenial cortex (coordinates: rostrocaudal −3.7, mediolateral 2.2, dorsoventral −3.5). Bipolar EEG signals were amplified and filtered (bandpass 0.1–75 Hz). An additional screw electrode was implanted in the frontal bone and used as ground.

For ATh unit recording, a 2-mm circular opening was made over the region of the ATh (coordinates: rostrocaudal −1.2 to −1.9, mediolateral 0.8 to 2.2, dorsoventral −4.8 to −7.5). A tungsten microelectrode (∼ 10 MΩ) was lowered through the opening to record unit activity from the ATh region. On average five units were recorded per animal. Unit activity was amplified, filtered (0.3–10 kHz), and acquired with an A/D 12-bit resolution (RC Electronics). Single units were isolated with a window discriminator (FHC, Bowdoinham, ME, USA) when a stable and reproducible waveform and/or a 4:1 or greater signal-to-noise ratio was observed. At the end of each experiment the rat was sacrificed with an overdose of anesthetic and immediately perfused with PBS followed by 10% formalin. Brains were cut on a freezing microtome. Sections (50 μm) were mounted on glass slides and stained with cresyl violet. Small electrolytic lesions made before the end of the experiment, and recording locations were later determined by histological analysis.

2.2 Methods of analysis

For each cell, a recording epoch consisted of 20- to 80-s continuous rhythmic (theta) activity induced by a gentle tail pinch. Two to four separate epochs were collected for each cell. For spectral analysis the data were digitally resampled at 200 Hz. The time series for each cell were divided into 60 trials of 256 points each. These trials were viewed as an ensemble of 60 independent realizations (trials) of the underlying stochastic process. For each EEG channel the ensemble mean was subtracted from each trial and the trial was then normalized by dividing the ensemble standard deviation. For the unit data each spike was converted into a shape similar to a Gaussian derivative and then filtered by using a zero-phase first-order lowpass Butterworth digital filter with a cutoff frequency at 30 Hz.

The squared coherence function between any two time series $x(t)$ and $y(t)$ is defined as

$$C_{xy}^2(f) = |S_{xy}(f)|^2 / S_{xx}(f) S_{yy}(f)\,,$$

where $S_{xx}(f)$ and $S_{yy}(f)$ are the power spectral density functions of $x(t)$ and $y(t)$, respectively, and $S_{xy}(f)$ is the cross-spectral density function between $x(t)$ and $y(t)$. For signals from three channels $x(t)$, $y(t)$, and $z(t)$, the partial coherence can be calculated from the auto- and cross spectra as

$$\gamma_{xy\cdot z}^2(f) = \frac{\left|S_{yx}(f)S_{zz}(f) - S_{yz}(f)S_{zx}(f)\right|^2}{(S_{yy}(f)S_{zz}(f) - \left|S_{yz}(f)\right|^2)(S_{xx}(f)S_{zz}(f) - |S_{xz}(f)|^2)}$$

(Bendat and Piersol 1986). Power spectral densities and ordinary coherence were pairwise computed using the function spectrum in MATLAB, which performs a standard Fourier spectral analysis of the two time series X and Y using a Hanning window. Partial coherence was then computed according to the equation above.

The variability of ordinary and partial coherence values was assessed using the bootstrap resampling technique

(Efron 1982; Efron and Tibshirani 1993). To perform a significance test, a "shuffled" control condition was created randomly from the data. Specifically, data for each of the three channels from different trials were put into a new synthetic trial. For the synthetic ensemble of such trials, the temporal structure for each individual channel was preserved, but their interdependence was removed based on the random trial combination. For each cell, 500 bootstrap resamples of such a synthetic ensemble were produced, creating a baseline distribution with which to compare the coherence values. The mean plus two standard deviations of ordinary coherence and partial coherence were then computed from the distribution across the bootstrap resamples of the synthetic ensemble to obtain a 95% confidence interval. Partial coherence values were considered statistically abolished when they fell below the 95% confidence level.

3 Results

We start by describing the potential confounding effects of noise in assessing directional influences (driving) in multivariate time series with partial coherence and Gersch Causality. We present heuristic arguments and test these arguments using numerical simulations. The biological data set is analyzed to provide evidence supporting the hypothesis.

3.1 Heuristic arguments

Suppose that there are three signals exhibiting strong pairwise coherence in a certain frequency (e.g., theta range). Let the three signals at that frequency be represented by

$$X_1 = \theta + \eta_1 ,$$
$$X_2 = \theta + \eta_2 ,$$
$$X_3 = \theta + \eta_3 .$$

Here the common variable θ reflects the fact that each channel contains a component that is coherent with the components of other channels, and η_i denotes independent local noise. We perform many independent trials. For each trial we collect values for X_1, X_2, and X_3. Our working assumption is that X_1 is correlated with X_2. To study the correlation between X_1 and X_2 after removing the effect of X_3, we carry out the following operation. Examine the entire collection of trials and select those trials where X_3 is roughly the same constant to form a subset of trials. For this subset of trials compute again the correlation between X_1 and X_2. This is the essence of partialling. If the correlation between X_1 and X_2 for the subset is zero, then we say that the original coherence is spurious and identify X_3 as the driver according to Gersch's idea (Gersch and Goddard 1970).

To see how this partialling operation is affected by the signal-to-noise ratio effect, let us imagine that η_3 is zero. When X_3 is held constant in this case, θ is held at the same constant value, since $X_3 = \theta$. For the subset of trials where θ is held constant, the variability in X_1 and X_2 is entirely due to the local noise η_1 and η_2. Thus the correlation between X_1 and X_2 after partialling out X_3 will be zero since η_1 and η_2 are assumed to be independent (Fig. 1). On the other hand, if η_3 is substantial compared with θ, then holding X_3 constant only means that the sum of θ and η_3 is a constant. The values of θ can still vary in X_1 and X_2, and this common variation is the reason that the partial correlation between X_1 and X_2 will not be zero.

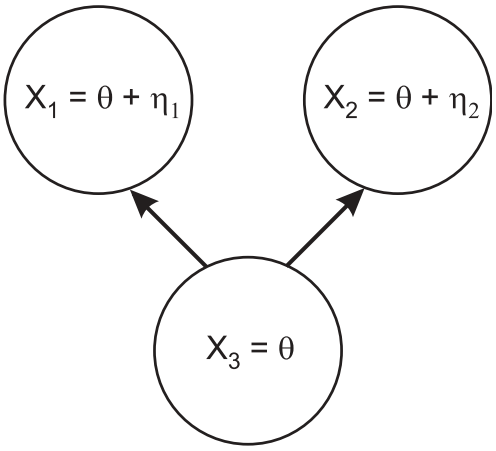

Fig. 1. Effect of noise on partial-coherence-based Gersch Causality. A schematic diagram with three random variables is used to illustrate how the partialling operation is affected by the signal-to-noise ratio effect. When η_3 is zero, holding X_3 at a constant value means that θ is held at the same constant value. The correlation between X_1 and X_2 after partialling out X_3 will be zero since η_1 and η_2 are assumed to be independent noise sources. If η_3 were not zero, then the value of θ could still vary in X_1 and X_2, and in that case this common variation would make the partial correlation between X_1 and X_2 nonzero

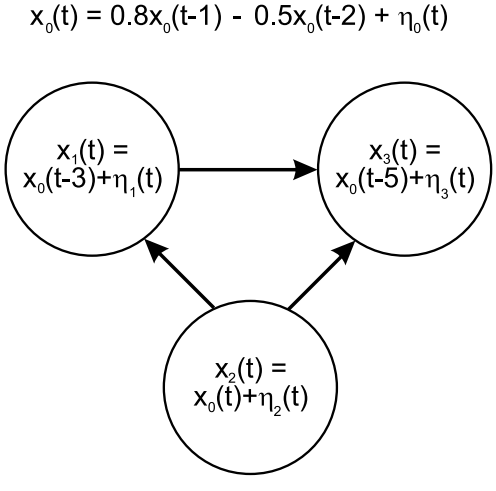

Fig. 2. The mathematical model used for the simulation. Data were generated with a simple second-order autoregressive model: $X_0(t) = 0.8X_0(t-1) - 0.5X_0(t-2) + \eta_0(t)$, where $\eta_0(t)$ is a Gaussian white noise with zero mean and standard deviation 1. We assume there are three recording sites (channels) X_1, X_2, and X_3, each of which contains a version of $X_0(t)$ with different delays and local additive noise. Specifically, X_1 receives the input from X_2 after a delay of three time units and X_3 receives the same input after a delay of five time units. X_3 can also be thought of as receiving an input from X_1 after a delay of two time units

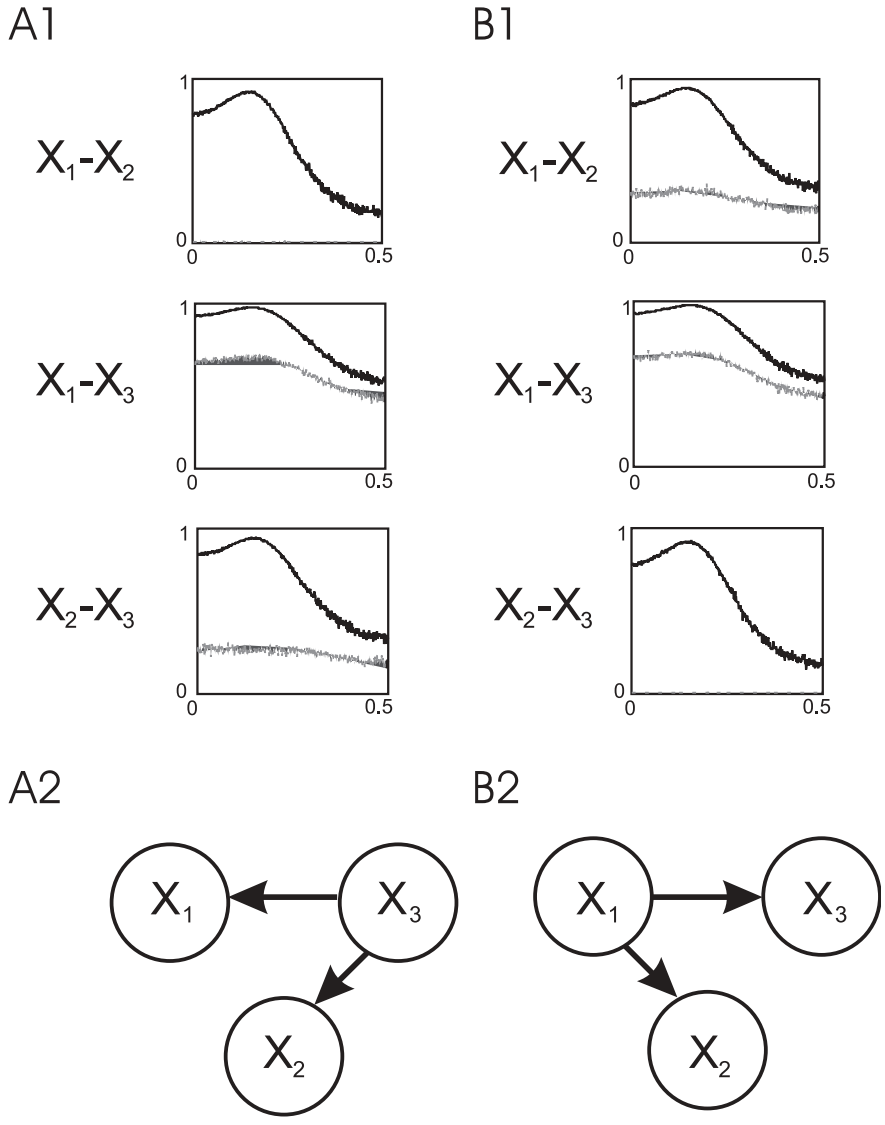

Fig. 3a, b. Results from simulation. Ordinary (*black solid lines*) and partial (*gray dotted lines*) coherences for the three distinct pairs of channels for both Case I and Case II are shown in **a1** and **b1**, respectively. For Case I (**a1**), we note that the noise-free channel X_3 is identified as the driver according to Gersch Causality since the coherence between X_1 and X_2 (*top panel*) disappears after partialling out X_3. The connectivity pattern based on this interpretation is shown in **a2**. For Case II (**b1**) the coherence between X_2 and X_3 (*bottom panel*) disappears by partialling out X_1, the noise-free channel, leading to X_1 being identified as the driver. The connectivity pattern in **b2** shows this conclusion

The foregoing discussion indicates that when a structure is identified as the driver in a multivariate situation, it may simply mean that the signal recorded from that site is the best representation (i.e., noise free) of the signal shared by all the recorded channels.

3.2 Numerical simulations

The ideas presented above are tested in simulations where the causal interactions are built into the model. We create the data by using a simple second-order autoregressive model. Let

$$X_0(t) = 0.8X_0(t-1) - 0.5X_0(t-2) + \eta_0(t)\,,$$

where $\eta_0(t)$ is a Gaussian white noise with zero mean and standard deviation one. Assume that there are three recording sites (channels) each of which contains a version of $X_0(t)$ with different delays and local additive noise. Specifically,

$$X_1(t) = X_0(t-3) + \eta_1(t)\,,$$
$$X_2(t) = X_0(t) + \eta_2(t)\,,$$
$$X_3(t) = X_0(t-5) + \eta_3(t)\,.$$

Here Channel 1 receives the input from Channel 2 after a delay of three time units. Channel 3 receives the same input after a delay of five time units. In a sense, Channel 3 also receives an input from Channel 1 after a delay of two time units. The connectivity patterns in this model can be summarized in Fig. 2. As indicated previously, partial coherence essentially identifies the driver as the channel with a nearly noise-free signal. To test this idea, we consider the following two cases.

For Case I, we let $\eta_3(t) = 0$, $\mathrm{var}(\eta_1(t)) = 0.04$, and $\mathrm{var}(\eta_2(t)) = 0.06$. Our theory predicts that $X_3(t)$ will be identified as the driver. Figure 3a1 shows the coherence (darker curves) between the indicated channels and the partial coherence between the same channel pair after removing the influence of the third channel. As expected, the partial coherence between X_1 and X_2 becomes zero, implicating $X_3(t)$ as the driver. The corresponding Gersch Causality pattern is shown in Fig. 3a2. For Case II, we let $\eta_1(t) = 0$, $\mathrm{var}(\eta_2(t)) = 0.06$, and $\mathrm{var}(\eta_3(t)) = 0.04$, and we predict that $X_1(t)$ will be identified as the driver. Figure 3b1 bears this prediction out, and the corresponding causal pattern according to the Gersch interpretation is shown in Fig. 3b2.

Both driving patterns in Fig. 3 are in contradiction with the true pattern in Fig. 2. We note that in no case is the true driver, Channel 2, identified as such because the local noise is never made zero. This example clearly demonstrates that partial-coherence-based causality measures are extremely sensitive to the presence of noise and thus are highly problematic in inferring directions of driving in biological applications when signal-to-noise ratios cannot be accurately determined a priori.

3.3 Experimental findings

In the following discussion, we illustrate the principles discussed above on a biological data set involving simultaneous recordings of EEG signals from the Hipp and RCx, and unit activity from the ATh. Results from two representative cells recorded from two different animals, referred to as R cell and K cell, are shown in Figs. 4 and 5. Figure 4 shows the power spectra from the three signals for R cell (left) and K cell (right). Clear peaks in the power spectra ~ 4 Hz are seen in the Hipp and RCx EEGs as well as in the unit recordings. R cell is characterized by having the greatest theta power for the Hipp channel, whereas K cell has the largest theta power for the RCx channel. ATh unit channels always have the lowest power among the three. This observation will become important for understanding the partial coherence results presented below in accordance with the theoretical ideas outlined above.

Figure 5 shows ordinary coherence (solid lines) and partial coherence (dashed lines) results for channel pairs RCx-Hipp (top panel), RCx-ATh (middle panel), and Hipp-ATh (bottom panel) for the two cells. The ordinary coherence is very high for all the channel pairs. For the R cell in Fig. 5a1, substantial partial coherence at theta frequency is evident between RCx-Hipp (top panel) (i.e., after partialling out the effect of the ATh unit). In like manner, there is pronounced coherence between Hipp-ATh (bottom panel) after partialling out the effect of RCx. However, partial coherence disappeared between RCx-ATh (middle panel) after removing the influence of Hipp. Thus, based on the principle of Gersch Causality, the hippocampus is identified as the driver of theta activity among the three structures studied. These findings are summarized in Fig. 5a2. For the K cell shown in Fig. 5b1, the ordinary coherence results are similar to those of the R cell. The partial coherence results, however, are very

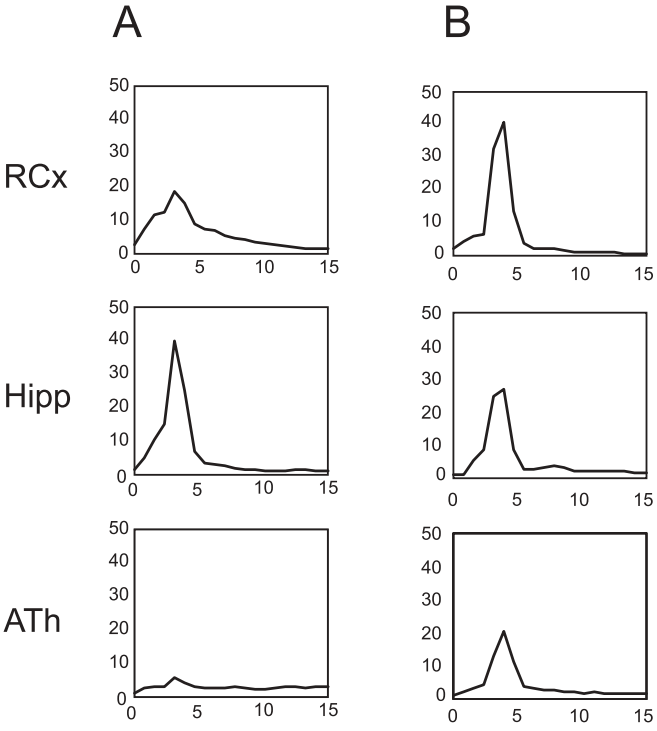

Fig. 4a, b. Power spectra for recordings of two representative cells, R cell (**a**) and K cell (**b**). *Top panels* show the power spectra from the RCx, the *middle panels* from the Hipp, and *bottom panels* from the two thalamic units (ATh). The two cells were recorded in two different animals. The unit of the vertical axis is μV^2 Hz

different. Specifically, the coherence between ATh and Hipp disappears after removing the influence of RCx, suggesting, according to Gersch Causality, that the cortex is the principal driver of Hipp and ATh theta activity for this cell. Figure 5b2 shows the connectivity pattern according to this interpretation.

We believe that the contradictory results in Fig. 5 are not a reflection of the true underlying connectivity pattern. They are the consequence of a signal-to-noise ratio as postulated in the heuristic discussion above. The power spectral results in Fig. 4 support this assertion. Specifically, for the R cell, the hippocampus has a much larger and sharper spectral peak in the theta range, indicating a relatively strong signal in that location. As expected, for this cell the hippocampus is identified as the driver. On the other hand, for the K cell the cortex has the largest power peak among the three signals, and it is thus identified as the driver by the partial coherence method. Further supporting evidence for the signal-to-noise ratio hypothesis comes from the fact that for all cells examined, we failed to encounter a single case in which the ATh unit was identified as the driver using partial coherence analysis. The reason appears quite obvious – the ATh single-unit activity signal, although showing theta rhythmicity, always has the lowest power when compared to the large EEG signals from the hippocampus and the cortex (Fig. 4).

To show that the signal-to-noise ratio effect in Figs. 4 and 5 is not an isolated phenomenon, we further analyzed data from 16 units showing strong coherence with hippocampal EEG. We refer to these units as "theta-rhyth-

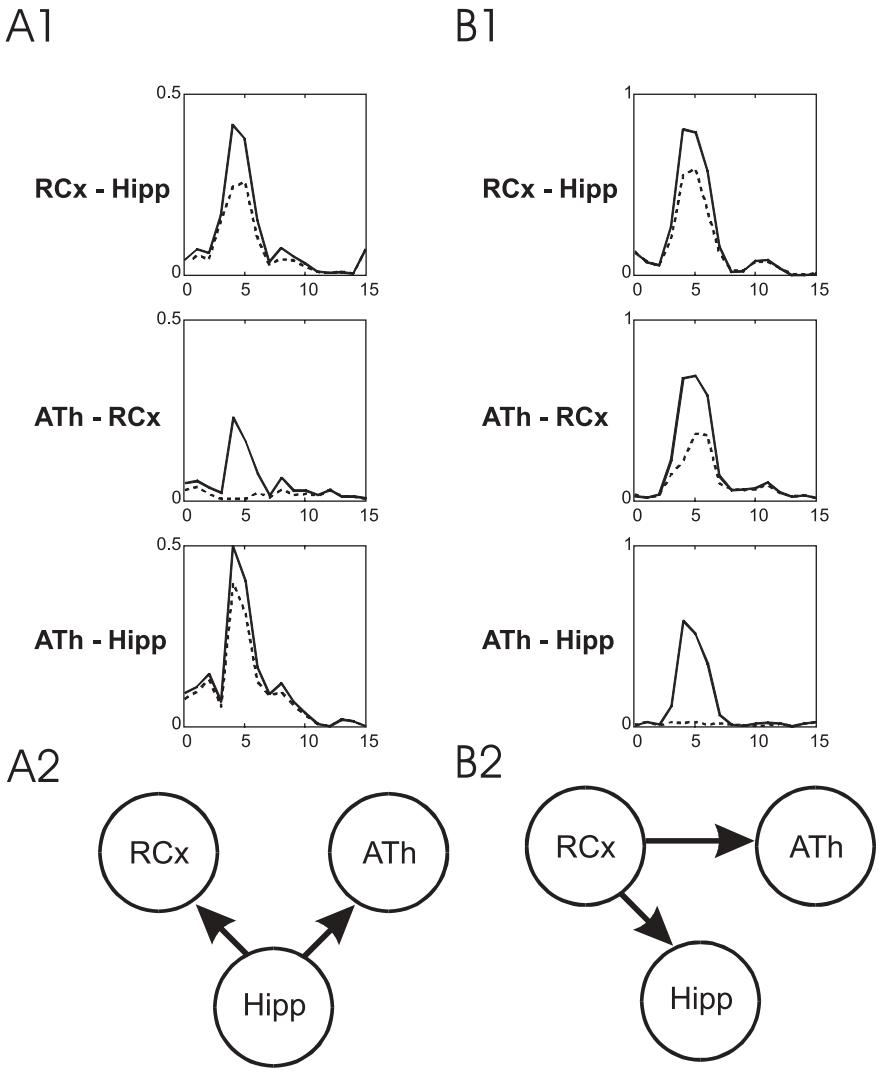

Fig. 5a, b. Ordinary and partial coherence for the recordings of two representative cells, R cell (**a**) and K cell (**b**). The *solid lines* in the *top panels* show the ordinary coherence between RCx and Hipp. The *dotted lines* show the partial coherence between RCx and Hipp after partialling out ATh. The *solid lines* in the *middle panels* show the ordinary coherence between ATh and RCx. The *dotted lines* show the partial coherence between ATh and RCx after statistically removing the influence of Hipp. The *solid lines* in the *bottom panels* show the ordinary coherence between ATh and Hipp. The *dotted lines* show the partial coherence between ATh and Hipp after removing RCx. Partial coherence identifies the hippocampus as the driver for the R cell (*middle panel* in **a1**) and the retrosplenial cortex as the driver for the K cell (*bottom panel* in **b1**). The corresponding Gersch Causality diagrams are shown in **a2** and **b2**, respectively

Table 1. Peak coherence of units in different anterior thalamic nuclei with hippocampal theta

Nuclei	AV	AD	AM
Peak coherence (Mean ± SD)	0.46 ± 0.16	0.34 ± 0.17	0.32 ± 0.10
Number of units (*n*)	12	2	2

mic" units. Most of these theta-rhythmic units ($n = 12$) were located in the anteroventral (AV) nucleus of ATh. Two units were located in the anterodorsal (AD) nucleus, and two units were located in the anteromedial (AM) nucleus. The average peak coherence between the units in each of these three nuclei and the corresponding hippocampal theta EEG are summarized in Table 1.

The heuristic arguments and the results in Figs. 4 and 5 suggest that the relative theta spectral power in the two EEG channels (Hipp and RCx) is a determining factor concerning which structure will be identified as the driver according to partial coherence. In Fig. 6 we examine partial coherence as a function of this relative power for all 16 cells. In Fig. 6a, the filled squares denote the variable, power(Hipp) / (power(Hipp) + power(RCx)), for each cell and the open squares are the partial coherence between RCx and ATh after removing the influence of Hipp. The filled triangles represent the variable, power(RCx) / (power(Hipp) + power(RCx)), for each cell. The partial coherence between Hipp and ATh after removing the influence of RCx is shown as open triangles. For 12 units (1–12), the hippocampus has a relatively high power, and as a consequence, the partial coherence between RCx and ATh is statistically abolished, implicating

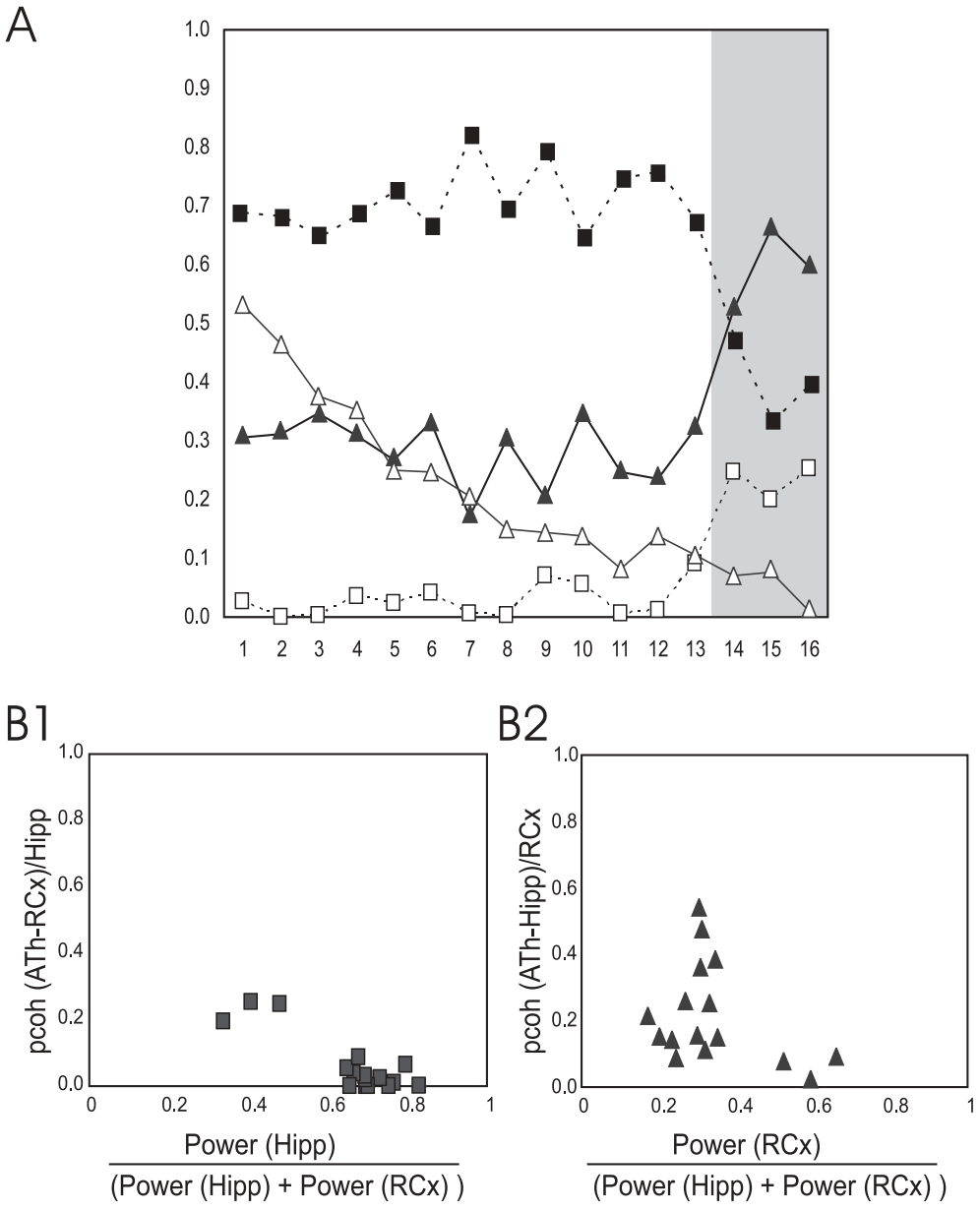

Fig. 6a, b. Relationship between relative power and partial coherence. **a** Normalized relative power for RCx (*filled triangles* connected by *solid black lines*) and for Hipp (*filled squares* connected by *dashed black lines*) for all theta-rhythmic cells studied (n = 16). Partial coherence between RCx and ATh after removing Hipp (*open squares* connected by *dashed lines*) and partial coherence between Hipp and ATh after partialling out RCx (*filled triangles* connected by *solid lines*). The shadowed area corresponds to the three cases where the relative power of the cortex becomes more predominant than the relative power of the hippocampus. **b** The same data shown differently. **b1** Partial coherence between RCx and ATh as a function of normalized relative power of hippocampus. **b2** Partial coherence between Hipp and ATh against normalized relative power of the cortex. Note that the R cell and K cell in Figs. 4 and 5 correspond to cell 2 and cell 16 in the present plots

Hipp as the driver. (The R cell in Figs. 4 and 5 is cell 2 here.) For cells 14–16, the relative theta power from RCx becomes greater than that from Hipp, and, as expected, the partial coherence between RCx and ATh increases significantly, whereas the partial coherence between Hipp and ATh declined substantially. For cell 16 (the K cell in Figs. 4 and 5), the partial coherence between Hipp and ATh is statistically abolished, implicating the retrosplenial cortex (RCx) as the driver.

To highlight the relation between the partial coherence and the relative power of the recording channel that has been partialled out, we replot the data in Fig. 6a in Fig. 6b1 and 6b2. Figure 6b1 displays the partial coherence between RCx and ATh after partialling out Hipp vs. the relative power of hippocampus. We note that as the power of the hippocampus signal increases, the partial coherence tends toward zero and the hippocampus becomes identified as the network driver. In Fig. 6b2, as the power of the

cortex becomes stronger, the partial coherence between Hipp and ATh diminishes to the point where the cortex becomes the driver.

4 Discussion

Partial coherence and the accompanying framework of interpretation in the form of Gersch Causality is a widely used technique for identifying sources of influence and causal relations in neurobiological multivariate recordings (Lopes da Silva et al. 1980; Turbes et al. 1983; Turbes and Schneider 1989; Kocsis and Vertes 1994; Halliday et al. 1995; Cohen et al. 1995; Sherman et al. 1997; Rosenberg et al. 1998; Kocsis et al. 1999; Mima et al. 2000; Larsen et al. 2000; Timmermann et al. 2003; Kubota et al. 2003). The result of the present work makes it clear that this approach is susceptible to noise contamination, questioning its usefulness in biological signal processing.

For our biological data, partial coherence analysis leads to contradictory results. For the two cells examined in Figs. 4 and 5, Gersch Causality led to the conclusion that in one case the hippocampus was the driver of theta activity for both the cortex and thalamus (R cell), whereas in the other case the cortex was the driver for the hippocampus and thalamus (K cell). The main difference between these two cells is that, for the R cell, power in the theta range for the hippocampus was the greatest among the three signals, whereas for the K cell, power in the theta range is the highest for the cortex. The population result of all 16 cells in Fig. 6 is also consistent with this idea.

In accordance with our heuristic arguments and simulations, we interpret the foregoing to indicate that the purer the signal (less noise), the greater its influence (driving) on simultaneously recorded signals in multivariate time series using partial coherence analysis. The consistent identification of the "strongest" signal as the driver may, however, not represent true causal or directional influences and, further, may not be easily reconciled with known anatomical and physiological data. For instance, it is well known that the hippocampus projects to the mammillary bodies (MB), the MB to the ATh, and the ATh in turn to the RCx. There are also direct projections from the hippocampus (subiculum) to the ATh (Swanson and Cowan 1977; Sikes et al. 1977). Based on these connections, the Hipp could serve as the driver for the ATh and RCx, and the ATh for the RCx, but it seems unlikely that the RCx is the driver of theta activity in both the Hipp and ATh as shown for the K cell by the partial coherence analysis. Thus, flaws in the methodology underlie the contradictory results seen in this case.

Causal influence is fundamentally a concept involving the temporal order of events. From its definition partial coherence incorporates no such information. This is another reason why partial coherence analysis is not suited for identifying causal influence or direction of driving. In recent years another way of assessing the causal relations between a pair of random time series stemming from the idea of Wiener (1956) has begun to receive attention in the neuroscience community (Bernasconi and Konig 1999; Liang et al. 2000; Baccala and Sameshima 2001; Kaminski et al. 2001). Acknowledging the importance of temporal ordering in the inference of causal relations from a purely statistical point of view, Wiener (1956) proposed that, for two simultaneously measured time series, one series can be called causal with respect to the other if we can better predict the second time series by incorporating the knowledge of the first one. This concept was later adopted and formalized by Granger (1969) in the context of linear regression models of stochastic processes. Evaluation of this technique using data from the theta-generating circuit is currently underway.

Acknowledgements. This work was supported by NIH, NSF, and ONR.

References

Albo Z, Viana Di Prisco G, Truccolo W, Vertes RP, Ding M (2001) A study of neural interactions within the limbic system using partial coherence and direct transfer functions analysis. Soc Neurosci Abstr 27: 630

Albo Z, Viana Di Prisco G, Vertes RP (2003) Anterior thalamic unit discharge profiles and coherence with hippocampal theta rhythm. Thalamus Related Sys 2:133–144

Baccala LA, Sameshima K (2001) Partial directed coherence: a new concept in neural structure determination. Biol Cybern 84:463–474

Bendat JS, Piersol AG (1986) Random data: analysis and measurement procedures. Wiley, New York

Bernasconi C, Konig P (1999) On the directionality of cortical interactions studied by structural analysis of electrophysiological recordings. Biol Cybern 81:199–210

Cohen MI, Yu Q, Huang WX (1995) Preferential correlations of a medullary neuron's activity to different sympathetic outflows as revealed by partial coherence analysis. J Neurophysiol 74:474–478

Efron B (1982) The jackknife, the bootstrap, and other resampling plans. SIAM, Philadelphia

Efron B, Tibshirani RJ (1993) An introduction to the bootstrap. Chapman & Hall, London

Fuller WA (1987) Measurement error models. Wiley, New York

Gersch W, Goddard GV (1970) Epileptic focus location: spectral analysis method. Science 169:701–702

Granger CWJ (1969) Investigating causal relations by econometric models and cross-spectral methods. Econometrica 37:424–438

Halliday DM, Rosenberg JR, Amjad AM, Breeze P, Conway BA, Farmer SF (1995) A framework for the analysis of mixed time series / point process data – theory and application to the study of physiological tremor, single motor unit discharges and electromyograms. Prog Biophys Mol Biol 64:237–278

Kaminski M, Ding M, Truccolo WA, Bressler SL (2001) Evaluating causal relations in neural systems: granger causality, directed transfer function and statistical assessment of significance. Biol Cybern 85:145–157

Kocsis B, Vertes RP (1994) Characterization of neurons of the supramammillary nucleus and mammillary body that discharge rhythmically with the hippocampal theta rhythm in the rat. J Neurosci 14:7040–7052

Kocsis B, Bragin A, Buzsaki G (1999) Interdependence of multiple theta generators in the hippocampus: a partial coherence analysis. J Neurosci 19:6200–6212

Kubota D, Colgin LL, Casale M, Brucher FA, Lynch G (2003) Endogenous waves in hippocampal slices. J Neurophysiol 89:81–89

Larsen PD, Lewis CD, Gebber GL, Zhong S (2000) Partial spectral analysis of cardiac-related sympathetic nerve discharge. J Neurophysiol 84:1168–1179

Liang H, Ding M, Nakamura R, Bressler SL (2000) Causal influences in primate cerebral cortex during visual pattern discrimination. Neuroreport 11:2875–2880

Lopes da Silva FH, Vos JE, Mooibroek J, Van Rotterdam A (1980) Relative contributions of intracortical and thalamocortical processes in the generation of alpha rhythms, revealed by partial coherence analysis. Electroencephalogr Clin Neurophysiol 50:449–456

Mima T, Matsuoka T, Hallett M (2000) Functional coupling of human right and left cortical motor areas demonstrated with partial coherence analysis. Neurosci Lett 287:93–96

Rosenberg JR, Halliday DM, Breeze P, Conway BA (1998) Identification of patterns of neural connectivity – partial spectra, partial coherence, and neuronal interactions. J Neurosci Methods 83:57–72

Sherman DL, Tsai YC, Rossell LA, Mirski MA, Thakor NV (1997) Spectral analysis of a thalamus-to-cortex seizure pathway. IEEE Trans Biomed Eng 44:657–664

Sikes RW, Chronister RB, White LEJ (1977) Origin of the direct hippocampus – anterior thalamic bundle in the rat: a combined horseradish peroxidase – Golgi analysis. Exp Neurol 57:379–395

Swanson LW, Cowan WM (1977) An autoradiographic study of the organization of the efferent connections of the hippocampal formation in the rat. In: DeFrance J (ed) The septal nuclei, pp 37–64

Timmermann L, Gross J, Dirks M, Volkmann J, Freund HJ, Schnitzler A (2003) The cerebral oscillatory network of parkinsonian resting tremor. Brain 126:199–212

Turbes CC, Schneider GT, Morgan RJ (1983) Partial coherence estimates of brain rhythms. Biomed Sci Instrum 19:97–102

Turbes CC, Schneider GT (1989) Directionality of neural signals in central nervous system neural networks. Biomed Sci Instrum 25:1–5

Vertes RP, Albo Z, Viana Di Prisco G (2001) Theta rhythmically firing neurons in the anterior thalamus: implications for the mnemonic function of Papez's circuit. Neuroscience 104(3):619–625

Wiener N (1956) The theory of prediction. Modern mathematics for engineers, Series 1, Beckenback EF, Ch 8